C.P. No. 1311

C.P. No. 1311

PROCUREMENT EXECUTIVE, MINISTRY OF DEFENCE

AERONAUTICAL RESEARCH COUNCIL

CURRENT PAPERS

Thrust/Drag Analysis for a Front Fan Nacelle having Two Separate Co-Axial Exhaust Streams

by

P. G. Street

National Gas Turbine Establishment

LONDON: HER MAJESTY'S STATIONERY OFFICE
1975
PRICE 90p NET

C.P. No.1311*
February 1973

THRUST/DRAG ANALYSIS FOR A FRONT FAN NACELLE HAVING TWO SEPARATE CO-AXIAL EXHAUST STREAMS

- by -
P.G. Street
National Gas Turbine Establishment

SUMMARY

The forces acting on and around a high by-pass ratio front fan nacelle have been considered in the light of the findings of an ARC panel on thrust and drag definitions for jet engines. From these considerations, thrust and drag components which take account of mutual interference have been defined.

A technique for defining an afterbody, or gas generator cowl drag in the presence of external flow is derived and the experimental measurements required are listed. Example calculations using experimental data are used to demonstrate the technique.

*Replaces NGTE Report 321 - A.R.C.34 645

CONTENTS

APPENDICES

ILLUSTRATIONS

1.0 Introduction

With the advent of the high by-pass ratio front fan engine as a commercial proposition, the problem of defining thrust and drag for a nacelle with two separate co-axial exhaust streams has become pressing. The problem is complicated by the fact that the flow from the outer, or fan exhaust passes over the surface of the downstream part of the nacelle, the afterbody. Thus the methods adopted for single stream nacelles, outlined in References 1 and 2, need modifying. Furthermore, the ideas need extending so that values of component thrusts and drags can be determined from experimental measurements.

As the specific thrust decreases with rising by-pass ratio the ratio of gross to net thrust increases. One feature of powerplants with a high ratio of gross to net thrust is a marked sensitivity to exhaust system performance. Losses in the exhaust system effectively act on the gross thrust level. For an engine of by-pass ratio 5, the ratio of gross to net thrust at cruise at a high subsonic Mach number is between $2\frac{1}{2}$ and 3/1. Thus a 1 per cent decrease in exhaust system performance would cost between $2\frac{1}{2}$ and 3 per cent on net installed performance.

This Report will show that the drag of the afterbody, where it is scrubbed by the fan jet, is properly treated as a loss of thrust, so that the loss is effectively magnified by the gross to net thrust ratio. The drag of the part of the nacelle upstream of the fan nozzle, the intake and fan cowl, can be treated by established methods so attention will be focussed on afterbody drag in the latter part of the Report.

It should be noted that the analysis which follows deals specifically with axisymmetric nacelles in isolation. The analysis should be used with caution in installations where the flow fields are likely to be non-symmetric.

2.0 Drag in potential flow

The drag of a closed non-lifting body in isolation in infinite potential flow is zero. This is the well-known d'Alembert's paradox. Prandtl[3] extended the paradox to show that bodies of semi-infinite or infinite extent in the streamwise direction also have zero drag in potential flow. The only forces acting in potential flow would be normal pressure forces; there would be no skin friction. Thus the walls of an infinitely long stream tube would experience no drag either outside, since the stream tube could represent an infinite body, or inside, since pressures on either side of a streamline are equal. However, if one considers a part of either a closed body or an infinite body, then the force due to normal pressures will in general be non-zero. Thus one can see that it is possible for a part of a body to experience a force which is not a drag force; the force would be cancelled by equal and opposite components elsewhere on the body.

3.0 Drag in real flow

All bodies in real flow exhibit drag. If the flow is subsonic, this drag comprises two components, the skin friction which is the integrated shear stress at the wall, and pressure or form drag arising from the modification of the pressure distribution due to boundary layer growth and, perhaps, breakaway of the flow from part of the surface.

When the flow is supersonic, an additional drag component, wave drag, further modifies the pressure distribution. The terms skin friction drag, form drag, profile drag and wave drag are discussed in more detail in Appendix II.

3.1 Drag of parts of bodies

As the drag in potential flow is zero, the pressure drag in real flow can be expressed as the difference between the integrated pressure force in real flow and the integrated pressure force in potential flow, considering the same body shape in both cases. This concept is useful when considering parts of bodies because, as stated above, the integrated pressure force on part of a body in potential flow would be non-zero. Thus the drag of part of a body is not the sum of the skin friction and the integrated pressure force. The pressure drag will be the difference between the non-zero integrated pressure force in potential flow and the integrated pressure force in real flow. The integrated pressure force in potential flow will be termed potential flow buoyancy in this Report. Its magnitude will clearly vary according to what portion of the whole body is being considered, tending to zero as the portion is extended to include the whole body.

4.0 Thrust and drag for a single stream nacelle

The ARC Panel, set up to consider 'thrust and drag definitions for ducted bodies and jet engines'[1,2], defined nacelle drag as the summation of forces on the outside of the stream tube bounding the flow which passes through the duct, and the thrust, or internal drag, as the summation of forces on the inside of the stream tube. These definitions are consistent because the stream tube is considered to extend from a station an infinite distance upstream from the duct inlet to a station an infinite distance downstream from the duct outlet. Thus the stream tube/body combination represents an infinite body which would have no drag in potential flow. The net force on the outer surfaces of the duct would not equal the drag because of potential flow buoyancy from the pre-entry and post-exit stream tubes. However, if all the forces are summed, then the potential flow buoyancy components cancel leaving the drag as the net result. A similar argument can be applied to the derivation of thrust.

Figure 1(a) shows a single stream nacelle in isolation. F_i and F_c* represent the total forces, skin friction plus normal pressure forces, on the external part of the intake and boat-tail respectively, the positive directions being taken as shown in the Figure. T_I is the intrinsic net thrust[1] comprising the summation of friction and pressure forces on the engine and internal parts of the duct. As all the forces have been included, the net installed thrust-minus-drag must equal $T_I + F_i - F_c$. Note, however, that F_i and F_c are forces, not drags.

The pre-entry and post-exit stream tubes have been included in Figure 1(b). Station 'o' is sufficiently far upstream for the static pressure to be undisturbed, i.e. upstream infinity, station 'i' is the

---

*All forces are taken to act in an axial direction. Lift is excluded. Symbols are defined in Appendix I.

plane of the intake, station 'e' is the nozzle exit plant and station 'j' is at downstream infinity where the static pressure once again reaches the undisturbed value.

The external drag, as defined in Reference 2, is the sum of the forces $F_{pre} + F_c - F_i - F_{post}$. If desired, this can be broken down into two components. These would be the intake drag, $F_{pre} - F_i$, which is equal to the sum of the datum intake drag and the basic spill drag as defined in Reference 2, and the boat-tail drag, $F_c - F_{post}$. This assumes that, strictly speaking, there is no interference between intake and boat-tail.

The internal thrust is the sum of the internal forces, $T_{pre} + T_I - T_{post}$. The net installed thrust 'X_n' is the thrust-minus-drag so that:-

$$X_n = T_{pre} + T_I - T_{post} - F_{pre} - F_c + F_i + F_{post} \quad ....(1)$$

However, forces on either side of a streamline must be equal so that:-

$$F_{pre} = T_{pre} \quad ....(2)$$

and

$$F_{post} = T_{post} \quad ....(3)$$

Combining Equations (2) and (3) with Equation (1)

$$X_n = T_I - F_c + F_i \quad ....(4)$$

which is the same result as was obtained by considering the forces on the hardware. But note that expressions for drag components are now available.

5.0 Thrust and drag for a two stream nacelle

Figure 2 shows a two stream nacelle with co-axial exhausts. The case treated here is the common one of a single intake, the flows being split within the engine. However, it is convenient for the analysis which follows to consider the intake flow as two separate flows, i.e. the internal flows maintain their separate identities throughout the flow field. Stations 'o', 'i' and 'j' are taken as before but two exhaust planes are now required, viz 'ef' and 'ep', representing the nozzle outlet planes for the by-pass, or fan flow and the gas generator, or primary flow respectively. Two intrinsic thrusts are specified, T_f and T_p, each representing a summation of forces within the duct, as before. T_f represents the summation of forces between stations 'i' and 'ef' on the annular stream tube which passes through the by-pass duct and T_p represents the summation of forces between stations 'i' and 'ep' on the inner stream tube bounding the gas generator flow.

Maintaining the definitions of thrust and drag given in References 1 and 2, external drag, D_{ext}, is defined by:-

$$D_{ext} = F_{pre} - F_i + F_c - F_{post} \quad ....(5)$$

The internal thrust of the fan stream, T_{int}, is given by:-

$$T_{int} = T_{pre} - f_{pre} + T_f - F_a - T_{post} + f_{post} \quad ....(6)$$

The internal thrust of the gas generator stream is given by:-

$$t_{int} = t_{pre} + T_p - t_{post} \quad ....(7)$$

The net installed thrust-minus-drag, X_n, is given by:-

$$X_n = T_{int} + t_{int} - D_{ext} \quad ....(8)$$

Substituting Equations (5), (6) and (7) into (8) and noting that forces on either side of streamlines are equal, as before, one can show that:-

$$X_n = T_f + T_p + F_i - F_c - F_a \quad ....(9)$$

In other words, the net installed thrust-minus-drag is equal to the algebraic sum of the internal forces and the external forces on the fan cowl and afterbody. Again following the method for the single stream nacelle, intake drag is equal to $F_{pre} - F_i$, cowl drag is equal to $F_c - F_{post}$ and afterbody drag could be taken as equal to $F_a - f_{post}$. A point to note is that F_a and f_{post} are internal forces. They modify the thrust of the fan and primary streams.

Whilst this is a viable definition of afterbody drag in that summation of thrusts and drags will give the correct net installed thrust-minus-drag, it omits to take account of the fact that the afterbody cannot reasonably be considered in isolation. Experimental results on certain geometries show the existence of potential flow buoyancy effects between the fan cowl and the gas generator afterbody. This takes the form of an apparent increase in cowl drag which is offset by an apparent reduction in afterbody drag. The mechanism of this buoyancy might be explained as follows. The external flow is directed towards the centreline as it leaves the cowl trailing edge and requires a pressure force to turn it back to an axial direction. This pressure force is a part of F_{post}. It is transmitted through the fan efflux thus raising the pressure level on the afterbody. The pressure levels on the cowl are lower than they would be if the afterbody were omitted. This may be further illuminated by the following example. Consider a case where the afterbody diameter is increased so that it effectively becomes a continuation of the cowl. Then the pressure distribution over

the cowl could be like the early part of the pressure distribution on a normal afterbody, i.e. a low pressure region. The pressure force on the latter part, the afterbody, would be positive, inducing a thrust nearly equal to the rearward force on the cowl.

Estimation of the bouyancy between the cowl and afterbody by calculation of the entire potential flow field would be extremely difficult. Assumptions of the relevant conditions at the fan nozzle throat would be open to question and, since the flow over the afterbody is supersonic, wave drag on the afterbody could not be excluded.

However, in Appendix II, the fact that drag always appears as a deficit in momentum flux in the wake is noted. Thus, if the drag of either the cowl or the afterbody could be estimated from conditions in the wake, then the difference between the drag and the net force on the body could be calculated. The drag of the afterbody is complicated by virtue of the three components - skin friction drag, form drag (or pressure drag due to boundary layer growth) and wave drag. Calculation of the sum of the first two components can be made using boundary layer prediction methods but the extension of this calculation to downstream infinity, i.e. allowing for the continued growth of the form drag in the wake is not at all well founded for supersonic flows and, since the difference in pressure levels between the afterbody trailing edge and free stream can be large, the correction term could also be large. No method is known for calculating the third component, wave drag, in this case.

However, if we turn our attention to the cowl, the situation is less clouded. The flow over the cowl afterbody is essentially subsonic so that the only contributions to drag are those due to boundary layer effects. Furthermore, the pressure level at the trailing edge of the cowl is not far different from the free stream static pressure. An additional bonus is that the pressure distribution is smooth in form; the pressure distribution on the afterbody is much more complicated due to the alternate expansion and compression regions. Thus the calculation of the momentum flux deficit in the cowl wake would be more reliable.

The thoughts expressed in the preceding paragraphs lead to the following technique for the derivation of afterbody drag from experimental measurements.

The force on the primary post-exit streamline, f_{post}, can be found by considering the change in momentum flux in the primary stream between stations 'ep' and 'j'. Thus:-

$$Q_p\left(V_{jp} - V_{ep}\right) = A_{ep}\left(P_{ep} - P_\infty\right) - A_{jp}\left(P_{jp} - P_\infty\right) - f_{post} \quad \ldots.(10)$$

where Q_p is the primary mass flow, V_{jp} is the primary stream velocity* at downstream infinity, V_{ep} is the velocity at outlet from the primary nozzle, A_{ep} is the primary nozzle outlet area, P_{ep} is the local static

---

*The derivation of V_j is further discussed in Section 5.3

pressure at the primary nozzle outlet, P_∞ is the free stream static pressure, A_{jp} is the area occupied by the expanded primary jet and P_{jp} is the pressure to which the primary jet expands. However, since station 'j' is at downstream infinity,

$$P_{jp} = P_\infty \qquad \ldots.(11)$$

and Equation (10) can be rewritten:-

$$f_{post} = Q_p \left(V_{ep} - V_{jp}\right) + A_{ep} \left(P_{ep} - P_\infty\right) \qquad \ldots.(12)$$

Then noting that the drag of the afterbody*, D_a, is equal to the momentum deficit in the wake at downstream infinity, one can write the momentum equation between station 'ef' and 'j' in the fan stream thus:-

$$Q_f \left(V_{jf} - V_{ef}\right) - D_a = A_{ef} \left(P_{ef} - P_\infty\right) - F_{post} + f_{post} - F_a \qquad \ldots.(13)$$

which can be re-arranged to give

$$F_{post} = Q_f \left(V_{ef} - V_{jf}\right) + A_{ef} \left(P_{ef} - P_\infty\right) + Q_p \left(V_{ep} - V_{jp}\right) + A_{ep} \left(P_{ep} - P_\infty\right) - F_a + D_a \qquad \ldots.(14)$$

However, the cowl boat-tail drag, D_c, is given by

$$D_c = F_c - F_{post} \qquad \ldots.(15)$$

Combining Equations (14) and (15)

$$F_c - D_c = Q_f \left(V_{ef} - V_{jf}\right) + A_{ef} \left(P_{ef} - P_\infty\right) + Q_p \left(V_{ep} - V_{jp}\right) + A_{ep} \left(P_{ep} - P_\infty\right) - F_a + D_a \qquad \ldots.(16)$$

---

*It is shown in Section 5.3 that D_a may include a thrust recovery term equal to a proportion of the potential divergent thrust at supercritical pressure ratios

so that

$$D_a = Q_f \left(V_{jf} - V_{ef}\right) - A_{ef} \left(P_{ef} - P_\infty\right) + Q_p \left(V_{jp} - V_{ep}\right) - A_{ep} \left(P_{ep} - P_\infty\right) + F_a + F_c - D_c \quad \ldots.(17)$$

This result can be demonstrated by an alternative method as follows. The gross thrust-minus-drag of the complete exhaust system can be derived in two ways, either by considering nozzle exit momenta and body forces or by considering momentum flux at downstream infinity.

Thus

$$T - D = Q_f V_{ef} + A_{ef} \left(P_{ef} - P_\infty\right) + Q_p V_{ep} + A_{ep} \left(P_{ep} - P_\infty\right) - F_c - F_a \quad \ldots.(18)$$

or

$$T - D = Q_f V_{jf} + Q_p V_{jp} - D_c - D_a \quad \ldots.(19)$$

Combining the two equations, one can write:-

$$D_a = Q_f \left(V_{jf} - V_{ef}\right) - A_{ef} \left(P_{ef} - P_\infty\right) + Q_p \left(V_{jp} - V_{ep}\right) - A_{ep} \left(P_{ep} - P_\infty\right) + F_a + F_c - D_c \quad \ldots.(20)$$

which is identical to Equation (17). All of the terms on the right hand side of this equation can be either measured or predicted. The following Sections describe methods for estimating the individual terms.

5.1 The nozzle flows

In Equation (20) the mass flow rates, Q_f and Q_p, are presumed to be known either from direct measurements, as in model tests, or from engine performance curves in full scale tests. Calculation of the mass flows from a knowledge of the nozzle discharge coefficients could lead to errors in some installations since, as demonstrated in the examples given in Section 6.0, the gas generator nozzle applied pressure ratio can be significantly lower than the exhaust pressure ratio so that the nozzle may be operating in the regime where discharge coefficient varies rapidly with changes in applied pressure ratio. In addition the effect of asymmetry in the installation may lead to a variation in base pressure around the nozzle exit plane. Thus the precise value of discharge coefficient may be difficult to determine.

5.2 Exit velocities

These problems associated with base pressure also lead to difficulties in satisfactorily defining exit velocities (V_{ep} or V_{ef}). In the examples exit velocities have been evaluated from the applied pressure ratio

based on mean values of the jet pipe total and base pressures. Reference 1 gives details of integral methods for determining exit velocity, but these depend on a more detailed knowledge of the exit plane flow field than is usually available.

5.3 Calculations of the V_j's

Both derivations assume that the V_j's are computed using a conservation process from the exit velocities and the differences in base pressures from ambient static pressure.

The concept of "thrust-minus-drag" is well understood and there is no doubt that the "thrust-minus-drag" can be expressed in terms of exit momenta and body forces as shown in Equation (18). However, the expression given in Equation (19) depends on defining the thrust which would be obtained in the absence of drag - here written as $Q_f V_{jf} + Q_p V_{jp}$ (thus Equation (19) could be taken as a definition of the total drag $D_c + D_a$). Therefore the calculation of the V_j's depends on evaluating the thrust at downstream infinity which would be obtained in the absence of drag.

When the flow in the jet is wholly subsonic, it would seem reasonable to expect the flow to expand adiabatically and isentropically from the nozzle exit pressure to the ambient static pressure. Thus a value for V_j based on the Jones thrust[1] might be expected.

When the flow in the jet is wholly supersonic it would be unreasonable to expect any more thrust at downstream infinity than exists at the nozzle exit because of shock losses in the jet. Thus a value for V_j based on the Standard thrust[1] would seem reasonable. This implies that, if the body is shaped so that some further external expansion takes place, then the additional thrust is credited to the body rather than to the internal thrust. This additional thrust, here termed thrust recovery, would be a proportion of the potential divergent thrust. Thus we see that D_a, as now defined, is not the afterbody drag when the fan nozzle pressure ratio is supercritical, but is equal to the afterbody drag minus the thrust recovery. This, of course, leads to the possibility of obtaining a negative value for D_a when the thrust recovery exceeds the afterbody drag.

In the case when the APR is subcritical and the EPR is supercritical it is suggested that V_j should be based on an isentropic expansion to sonic conditions with no thrust change in the supersonic part of the jet. This has the advantage that the definition of thrust is continuous as pressure ratio is changed.

5.4 Calculation of the cowl and afterbody forces, F_c and F_a

The force on the cowl, or afterbody, is given by

$$F = \int_0^x 2\pi r \tau dx - \int_A \left(P_L - P_\infty\right) dA \qquad \ldots.(21)$$

taking boat-tail projected areas as positive.

The second integral in Equation (21) is determined directly from the pressure distribution. The first integral depends on a prediction of shear stress τ.

In Reference 7, Art 27.5, Shapiro suggests that flat plate skin friction data are fitted within ±2 per cent by*

$$C_{D\infty} = \frac{0.472}{\left(\text{Log}_{10}(R_\infty)\right)^{2.58} \left(1 + \frac{\gamma - 1}{2} M_\infty^2\right)^{0.467}} \quad \ldots.(22)$$

and

$$C_{F\infty} = C_{D\infty}\left(1 - \frac{1.12}{\text{Log}_{10}(R_\infty)}\right) \quad \ldots.(23)$$

In order to take into account pressure gradients, the length used in computing R_∞ should be replaced by the equivalent length 'X' defined in Equation (31) below, i.e. replace $R\infty$ by Rx.

Now,

$$\tau = C_{F\infty} \times \tfrac{1}{2} \rho_e V_e^2 \quad \ldots.(24)$$

Combining Equations (22), (23) and (24) and taking $\gamma = 1.4$, we can write

$$\tau = \frac{0.7\ P_L\ M_e^2 \times 0.472 \left(1 - \frac{1.12}{\text{Log}_{10}(Rx)}\right)}{\left(\text{Log}_{10}\ (Rx)\right)^{2.58} \left(1 + \frac{M_e^2}{5}\right)^{0.467}} \quad \ldots.(25)$$

Now we can re-write Equation (21) as

$$F = 0.6608\pi \int_0^x \frac{r\ P_L\ M_e^2 \left(1 - \frac{1.12}{\text{Log}_{10}(Rx)}\right)}{\left(\text{Log}_{10}\ (Rx)\right)^{2.58} \left(1 + \frac{M_e^2}{5}\right)^{0.467}} dx - \int_A \left(P_L - P_\infty\right) dA \quad \ldots.(26)$$

Thus, using Equation (26), one can estimate F_c and F_a. Whilst the estimation of F_c should be fairly accurate, the estimation of F_a will be less so. A direct measurement of F_a, if this is possible, would be preferable.

---

*∞ in this context means at the edge of the boundary layer

5.5 Calculation of cowl drag, D_C

It would be possible to calculate the boundary layer development along the cowl surface from the measured static pressure distribution, so that the boundary layer momentum thickness, θ_{TE}, at the trailing edge could be calculated. One could then calculate the momentum deficit at the trailing edge from:-

$$D = \rho_{TE} V_{TE}^2 2\pi r_{TE} \theta_{TE} \quad \ldots.(27)$$

However, D would not equal the drag D_C since, while the first term of Equation (II.11) of Appendix II is zero in the wake, the second term may continue to grow. A method of accounting for the continued activity of the last term is to use the momentum thickness at downstream infinity rather than at the trailing edge. An exact analytical technique for calculating the momentum thickness at downstream infinity does not exist, but Squire and Young[4] have developed a semi-empirical method for incompressible flow which has been extended by Nash et al[5] for compressible flow. Nash's result is:-

$$\frac{\theta_\infty}{\theta_{TE}} = \left(\frac{V_{TE}}{V_\infty}\right)^{\frac{\bar{H}+5}{2}} \times \left(\frac{\Theta_{TE}}{\Theta_\infty}\right)^3 \quad \ldots.(28)$$

where $\bar{H}$ is the transformed shape parameter; a value for $\bar{H}$ of 1.4 is suggested, θ_∞ is the momemtum thickness at downstream infinity, V_∞ is the undisturbed free stream velocity and Θ is the static temperature.

Thus the total drag of the fan cowl due to boundary layer growth can be written:-

$$D_C = 2\pi r_{TE} \theta_{TE} \rho_\infty V_\infty^2 \left(\frac{V_{TE}}{V_\infty}\right)^{\frac{\bar{H}+5}{2}} \left(\frac{\Theta_{TE}}{\Theta_\infty}\right)^3 \quad \ldots.(29)$$

Since the static pressure at the trailing edge of the cowl is not far different from the free stream static pressure, the 'Nash' correction term will have a value close to unity.

The momentum thickness at the trailing edge can be predicted by the method of Reference 6. This method has been chosen simply to illustrate the technique. The quality of experimental data likely to be obtained may not justify more refined methods of boundary layer prediction. Stratford and Beavers' analysis is simple to carry out and gives results which are in fair agreement with later methods, particularly so far as θ prediction is concerned.

Summarising the method, the function $\bar{P}$, where

$$\bar{P} = \left[\frac{M}{1 + \frac{M^2}{5}}\right]^4 \quad \ldots.(30)$$

and the radius, r, are tabulated as functions of x. The equivalent length, X, is then evaluated, where

$$X = \left(\bar{P}r^{\alpha}\right)^{-1} \int_{0}^{x} \bar{P}r^{\alpha}\, dx \qquad \ldots.(31)$$

given $\alpha = 1.25$ if Rx is of order 10^6, and

$\alpha = 1.2$ if Rx is of order 10^7.

To assist in the evaluation of Equation (26), values of X should be tabulated along the surface. The Reynolds number at the trailing edge, Rx, is then evaluated from

$$Rx = \frac{4.71 \times 10^4 \times M \times X \times P_T \times \left(\Theta_T + 117 \times \left(1 + \frac{M^2}{5}\right)\right)}{\Theta_T^2 \times \left(1 + \frac{M^2}{5}\right)^{2.5}} \qquad \ldots.(32)$$

where X is in metres, P_T is in N/m^2 and Θ_T is in K. Then, according to Reference 6, if Rx is of order 10^6

$$\theta = 0.036 \left(1 + \frac{M^2}{10}\right)^{-0.70} X\, Rx^{-\frac{1}{5}} \qquad \ldots.(33)$$

and if Rx is of order 10^7

$$\theta = 0.022 \left(1 + \frac{M^2}{10}\right)^{-0.70} X\, Rx^{-\frac{1}{6}} \qquad \ldots.(34)$$

Having calculated θ at the trailing edge, D_c can be evaluated from Equation (29) which can be re-written in a more convenient form as

$$D_c = 2.8\pi\, r_{TE}\, \theta_{TE}\, P_{\infty}\, M_{\infty}^2 \left(\frac{M_{TE}}{M_{\infty}}\right)^{3.2} \left(\frac{1 + \frac{M_{\infty}^2}{5}}{1 + \frac{M_{TE}^2}{5}}\right)^{4.6} \qquad \ldots.(35)$$

5.6 Experimental measurements required

From Equation (20), the measurements required to determine D_a are listed below:

(a) Total pressure in the two exhaust streams and in free stream.
(b) The base pressures of the two nozzles.
(c) The static pressure in the free stream.

(d) The static pressure distribution on the fan cowl (from which both F_c and D_c can be calculated; see Sections 5.4 and 5.5).
(e) The force on the afterbody (or, as second best, the pressure distribution so that F_a may be computed; see Section 5.4).
(f) All projected and nozzle exit areas.
(g) The two nozzle flows.

6.0 Example calculations

Data for these example calculations can be found in Appendix III. The three test points are used to illustrate the three different methods required for the calculation of the V_j's. First, however, the calculations for F_a, F_c and D_c are discussed as these are common to all three examples.

6.1 A supercritical case

In Example 1 (Appendix III) both pressure ratios for the two nozzles are supercritical. Therefore, following Section 5.3, the gauge stream thrusts at the nozzle exits are taken as equal to the gauge stream thrusts at downstream infinity and Equation (20) can be re-written as:-

$$D_a = F_a + F_c - D_c \qquad \ldots.(36)$$

so that following Appendix III,

$$D_a = 2.74 + 6.31 - 4.98$$

$$= 4.07$$

Expressed as a proportion of the ideal gross gauge convergent thrust of the two nozzle streams separately expanded,

$$\frac{D_a}{F_{ID}} = 0.0064$$

6.2 An intermediate case

In Example 2, both pressure ratios for the fan nozzle are supercritical, but, while the EPR for the primary nozzle is supercritical, the APR is subcritical. In this case, the change in stream thrust in the fan stream is taken as zero, but the change in the primary stream is taken as that from the APR to sonic conditions.

Thus Equation (20) can be re-written as:-

$$D_a = Q_p \left(V_p^* - V_{ep}\right) - A_{ep} \left(P_{ep} - P_\infty\right) + A_p^* \left(P_p^* - P_\infty\right) + F_a + F_c - D_c \qquad \ldots.(37)$$

A more convenient form of Equation (37) is:-

$$D_a = \left(Q\sqrt{\Theta_T}\right)_p \left[\left(\frac{V}{\sqrt{\Theta_T}}\right)^*_p - \left(\frac{V}{\sqrt{\Theta_T}}\right)_{ep}\right] - P_{Tp} A_{ep} \left[\frac{P_{ep}}{P_{Tp}} - \left(1 - \frac{A_p^*}{A_{ep}}\right)\frac{P_\infty}{P_{Tp}} - \frac{A_p^*}{A_{ep}}\frac{P_p^*}{P_{Tp}}\right] + F_a + F_c - D_c \quad \ldots.(38)$$

or

$$D_a = \left(Q\sqrt{\Theta_T}\right)\left\{18.48 - \left(\frac{V}{\sqrt{\Theta_T}}\right)_{ep}\right\} - P_{Tp} A_{ep}\left\{\frac{1}{APRP} - \left(1 - \frac{A_p^*}{A_{ep}}\right)\frac{1}{EPRP} - \frac{A_p^*}{A_{ep}} \times 0.52828\right\} + F_a + F_c - D_c \quad \ldots.(39)$$

so that $D_a = 3.23 - 3.44 - 2.28 + 7.54 - 4.97$

$= 0.08$

and $\frac{D_a}{F_{ID}} = 0.00016$

6.3 A subcritical case

Example 3 is typical of a case where the pressure ratios are subcritical. In this example, Equation (20) is used in full. Again for convenience, Equation (20) may be re-written as:-

$$D_a = \left(Q\sqrt{\Theta_T}\right)_f \left(\left(\frac{V}{\sqrt{\Theta_T}}\right)_{EPRF} - \left(\frac{V}{\sqrt{\Theta_T}}\right)_{APRF}\right) - P_{Tf}\, A_{ef} \left(\frac{1}{APRF} - \frac{1}{EPRF}\right)$$

$$+ \left(Q\sqrt{\Theta_T}\right)_p \left(\left(\frac{V}{\sqrt{\Theta_T}}\right)_{EPRP} - \left(\frac{V}{\sqrt{\Theta_T}}\right)_{APRP}\right) - P_{Tp}\, A_{ep} \left(\frac{1}{APRP} - \frac{1}{EPRP}\right)$$

$$+ F_a + F_c - D_c \qquad \ldots.(40)$$

so that

$$D_a = 7.16 + 9.39 - 7.41 - 10.13 - 2.10 + 9.01 - 4.97$$

$$= 0.95$$

and

$$\frac{D_a}{F_{ID}} = 0.003$$

7.0 Discussion

The final equation for "afterbody drag" is:-

$$D_a = Q_f \left(V_{jf} - V_{ef}\right) - A_{ef} \left(P_{ef} - P_\infty\right)$$

$$+ Q_p \left(V_{jp} - V_{ep}\right) - A_{ep} \left(P_{ep} - P_\infty\right) + F_a + F_c - D_c \qquad \ldots.(20\ bis)$$

As shown in Section 5.3, the methods of estimating V_j lead, in some circumstances, to a negative value for D_a when the thrust recovery exceeds the drag. The opinion has been advanced that the afterbody should be credited with any thrust recovery. It would be equally reasonable, however, to suggest that the afterbody should always be expected to produce the full thrust recovery and that any shortfall in this respect should be added to the afterbody drag. This would mean that, at supercritical exhaust pressure ratios, the velocity at downstream infinity, V_j, should be the fully expanded (convergent-divergent) value.

The choice between the two methods clearly represents a choice between two different scales to represent D_a, the first benefitting the

afterbody with any external expansion and treating the fan nozzle correctly, the latter penalising the afterbody for any failure to achieve thrust recovery.

The author can see no real reason for preferring one method to the other. Both approaches would give the same overall thrust-minus-drag - they merely vary the distribution of losses between the internal thrust and the afterbody drag.

It has not been found possible to separate the two components of D_a because the proportion of the potential thrust recovery actually achieved is not known. No absolute value of afterbody drag has been revealed in this Report. Rather the work should be read as a definition of a DRAG-MINUS-THRUST term, D_a, closely related to afterbody drag.

8.0 Conclusions

Thrust and drag for a nacelle having two separate co-axial exhaust streams have been analysed and a method has been developed for the determination of an afterbody drag term from experimental measurements. It has been shown that the drag of the afterbody is properly treated as a loss of gross thrust.

Inherent in the analysis are definitions of all component drags. The difference between the force on a component and the drag contribution of that component is highlighted.

The main purpose of this type of analysis is that it enables attention to be focussed on the component of the nacelle having the highest drag. It also enables comparisons to be made between different afterbodies on a given nacelle and can reveal any changes in, say, cowl drag caused by changes in the afterbody shape.

The technique is illustrated by typical examples using model data showing the use of the three definitions of momentum flux at downstream infinity.

ACKNOWLEDGEMENT

The author would like to thank his colleagues at Rolls-Royce and in the Ministry of Technology for the many useful discussions which lead to the final form of this Report.

REFERENCES

No.	Author(s)	Title, etc.
1		Report of the Definitions Panel on the definitions of the thrust of a jet engine and of the internal drag of a ducted body ARC CP190, 1955
2		Report of the Definitions Panel on definitions to be used in the description and analysis of drag ARC CP369, 1958
3	L. Prandtl	The mechanics of viscous fluids in 'Aerodynamic Theory' Vol. 3 edited by W. F. Durand 1935
4	H. B. Squire A. D. Young	The calculation of the profile drag of aerofoils ARC R and M 1838, November 1937
5	J. F. Nash J. Osborne A. G. J. Macdonald	A note on the prediction of aerofoil profile drag at subsonic speeds NPL Aero Report 1196, June 1966
6	B. S. Stratford G. S. Beavers	The calculation of the compressible turbulent boundary layer in an arbitrary pressure gradient - a correlation of certain previous methods ARC R and M No. 3207, September 1959
7	Ascher H. Shapiro	The dynamics and thermodynamics of compressible fluid flow, Vol. II The Ronald Press Company, New York 1954

APPENDIX I

List of symbols

A	projected area
APRF	fan stream applied pressure ratio $\frac{P_{Tf}}{P_{ef}}$
APRP	primary stream applied pressure ratio $\frac{P_{Tp}}{P_{ep}}$
α	exponent in formula for X
C_D	drag coefficient
C_F	skin friction coefficient
D	drag
D_a	afterbody drag-minus-thrust recovery
EPRF	fan stream exhaust pressure ratio $\frac{P_{Tf}}{P_\infty}$
EPRP	primary stream exhaust pressure ratio $\frac{P_{Tp}}{P_\infty}$
F,f	force
F_{ID}	gross ideal convergent thrust of two streams separately expanded
γ	ratio of specific heats
$\bar{H}$	transformed shape parameter
M	Mach number
P	static pressure
P_T	total pressure
$\bar{P}$	$\left(\frac{M}{1 + \frac{M^2}{5}}\right)^4$
Q	mass flow rate
r	radius
R_∞	Reynolds number referred to conditions at edge of boundary layer
Rx	Reynolds number based on X

S distance along surface

T,t thrust

Θ static temperature

Θ_T total temperature

θ momentum thickness

τ shear stress

V velocity

X equivalent length of boundary layer growth $X = \left(\bar{P}r^{\alpha}\right)^{-1} \int_0^X \bar{P}r^{\alpha} dx$

X_n net thrust-minus-drag

x axial distance

y distance normal to x axis

ρ density

δ^* displacement thickness

ψ $P_L - P_\infty$

β angle of surface relative to axis

$$\xi = \frac{r\, P_e M_e^2 \left(1 - \frac{1.12}{\mathrm{Log}_{10}(Rx)}\right)}{\left(\mathrm{Log}_{10}(Rx)\right)^{2.58} \left(1 + \frac{M_e^2}{5}\right)^{0.467}}$$

Suffices

a afterbody

b base

c cowl boat-tail

e edge of boundary layer

ef fan exit plane

ep primary exit plane

ext external

f fan stream

Fm	form
I	intrinsic
i	intake
int	internal
jf	fan at downstream infinity
jp	primary at downstream infinity
L	local static
p	primary stream, profile
post	post exit streamline
pre	pre-entry streamline
TE	trailing edge
w	wave
∞	undisturbed free stream condition
ϕ	friction

Superfix

*	at sonic conditions

APPENDIX II

Drag components

In two-dimensional flow we can write:-

$$\text{Pressure drag on a complete body} = \int_0^\infty \left(P - P_\infty\right) \frac{dy}{dx}\, dx \quad \ldots.(II.1)$$

and assuming δ^* is measured normal to the x axis,

$$\text{Pressure drag on displacement surface} = \int_0^\infty \left(P - P_\infty\right) \frac{d(y + \delta^*)}{dx}\, dx \quad \ldots.(II.2)$$

so that:-

(the pressure drag on the displacement surface) -

$$\text{(the pressure drag on the body)} = \int_0^\infty \left(P - P_\infty\right) \frac{d\delta^*}{dx}\, dx \quad \ldots.(II.3)$$

The drag of a complete body in isolation in potential flow is zero, so that the drag of the displacement surface is zero. Thus we can re-write Equation (II.3) as

$$\text{Zero - body pressure drag} = \int_0^\infty \left(P - P_\infty\right) \frac{d\delta^*}{dx}\, dx \quad \ldots.(II.4)$$

so that

$$\text{Body pressure drag} = \text{form drag} = -\int_0^\infty \left(P - P_\infty\right) \frac{d\delta^*}{dx}\, dx \quad \ldots.(II.5)$$

The above derivation can be transposed to axisymmetric flow to give:-

$$\text{Form drag, } D_{Fm} = -\int_0^\infty 2\pi r \left(P - P_\infty\right) \frac{d\delta^*}{dx}\, dx \quad \ldots.(II.6)$$

Alternatively, working from the boundary layer momentum equation[3], the pressure drag due to boundary layer growth can be derived as:-

$$D_{Fm} = \int_0^\infty 2\pi r\, \delta^* \frac{dP}{dx}\, dx \quad \ldots.(II.7)$$

which is the same as Equation (II.6) since, in general

$$\int y\,dx = -\int x\,dy \qquad \ldots.(II.8)$$

Skin friction

Skin friction arises from tangential shear stress at the surface of the body. If shear stress is represented by τ, then the local shear force on the body is $\tau\,dS$ and the axial component is $\tau\,dS\cos\beta$, where β is the angle of the surface relative to the axis.

Now,

$$dS\cos\beta = dx \qquad \ldots.(II.9)$$

so that the axial component of local shear force is $\tau\,dx$ and the total drag in two-dimensional flow due to skin friction is $\int_o^x \tau\,dx$.

In axisymmetric flow, the skin friction drag D_ϕ can be written:-

$$D_\phi = \int_o^x 2\pi r\,\tau\,dx \qquad \ldots.(II.10)$$

Profile drag

Profile drag, sometimes known as boundary layer drag, is the total drag due to boundary layer growth and thus equals the sum of the skin friction and form drags.

$$\text{Profile drag, } D_p = \int_o^x 2\pi r\,\tau\,dx - \int_o^\infty 2\pi r\left(P - P_\infty\right)\frac{d\delta^*}{dx}\,dx \qquad \ldots.(II.11)$$

Wave drag

When the flow over the afterbody is supersonic, the jet efflux will contain shock waves which, through the loss of total pressure, give rise to drag. The flows under consideration differ from those pertaining to supersonic aircraft because the flow over the afterbody is a supersonic jet surrounded by a subsonic flow field, rather than an infinite supersonic field. By way of explanation of the difference, first consider the boat-tail of a long fuselage in a supersonic flow field with no boundary layers. As the flow expands round the boat-tail, the velocity will increase - leading to sub-ambient pressures on the boat-tail surface. At the end of the boat-tail, the flow is suddenly straightened by a shock wave which extends out to infinity in the radial direction. The wave drag of the boat-tail is equal to the loss of momentum through this single infinite shock, which will equal the pressure integral over the boat-tail.

$$D_w = -\int_A \left(P - P_\infty\right) dA \qquad \ldots.(II.12)$$

In the case of the front fan nacelle afterbody, instead of the single shock extending out to infinity, neglecting viscous effects at the jet boundary, there are an infinite number of bounded shocks in the jet. The momentum loss in this infinite number of shocks is the wave drag which will in the absence of interference again equal the pressure integral over the afterbody. In the presence of a boundary layer, the wave drag is the wave drag of the displacement surface.

APPENDIX III

Example calculations

1.0 Definition of geometry

1.1 Fan cowl

TABLE I

	Static No.	x mm	r mm	dx mm	dA_{proj} mm^2
Limit	1	0	57.21	4.57	0
↑	2	9.14	57.21	9.14	0
	3	18.28	57.21	9.14	54.84
	4	27.43	56.90	9.14	129.36
	5	36.57	56.48	9.14	204.52
Limits of integration	6	45.72	55.75	9.14	297.43
	7	54.86	54.78	9.14	358.08
	8	64.00	53.67	9.14	437.44
	9	73.15	52.18	9.14	490.99
	10	82.29	50.67	9.14	499.06
	11	91.44	49.04	8.76	497.44
↓	12	99.82	47.44	4.95	302.59
Limit	T.E	100.58	47.24	-	-

1.2 Afterbody

TABLE II

	Static No.	x mm	r mm	dx mm	dA_{proj} mm^2
Limit	1	- 4.06	33.70	3.35	53.55
↑	2	2.61	33.19	6.68	123.87
	3	9.29	32.51	6.68	158.07
	4	15.97	31.64	6.68	183.88
	5	22.65	30.65	6.68	200.65
Limits of integration	6	29.33	29.56	6.68	218.72
	7	36.01	28.29	6.68	236.78
	8	42.69	26.89	6.68	250.33
	9	49.37	25.32	6.68	256.14
	10	56.05	23.67	6.68	260.01
↓	11	62.73	21.81	10.79	405.83
Limit	T.E	70.18	19.71	-	-

A_{ep} = 1132.3 mm^2 A_{ef} = 3450.5 mm^2

2.0 Example 1 - Supercritical pressure ratio readings

Tunnel	P_T	=	100.82 KN/m^2 abs	Θ_T	=	288 K
Fan stream	P_{Tf}	=	162.86 KN/m^2 abs	Θ_T	=	291 K
Primary stream	P_{Tp}	=	161.43 KN/m^2 abs	Θ_T	=	291 K
Fan nozzle base	P_{bf}	=	65.55 KN/m^2 abs			
Primary nozzle base	P_{bp}	=	74.84 KN/m^2 abs			
Free stream static	P_∞	=	62.84 KN/m^2 abs			

so that

$$APRF = 2.484$$

$$EPRF = 2.592$$

$$APRP = 2.157$$

$$EPRP = 2.569$$

$$M_\infty = 0.851$$

Pressure distributions

Fan Cowl		Afterbody	
Static No.	P_L in. KN/m^2 abs	Static No.	P_L in. KN/m^2 abs
1	63.39	1	95.94
2	61.02	2	73.76
3	59.60	3	58.58
4	58.92	4	48.09
5	58.24	5	49.00
6	58.31	6	53.54
7	59.60	7	70.1
8	59.60	8	73.09
9	62.64	9	67.73
10	63.29	10	54.52
11	68.13	11	69.42
12	68.13		

$$\left(Q\sqrt{\Theta_T}\right)_{FAN} = 22.24$$

$$\left(Q\sqrt{\Theta_T}\right)_{PRIM} = 7.17$$

$$F_{ID} = 641.77 \text{ N}$$

A full tabulation of the steps in calculating F_c, D_c and F_a are given in this example only.

2.1 Calculation of F_c

$$F_c = 0.6608 \int_0^x \frac{r\, P_L\, M_e^2 \left(1 - \frac{1.12}{\mathrm{Log}_{10}(Rx)}\right) dx}{\left(\mathrm{Log}_{10}(Rx)\right)^{2.58} \left(1 + \frac{M_e^2}{5}\right)^{0.467}} - \int_A \left(P_L - P_\infty\right) dA \quad \ldots.(26\ \text{bis})$$

Let $$\frac{r\, P_L\, M_e^2 \left(1 - \frac{1.12}{\mathrm{Log}_{10}(Rx)}\right)}{\left(\mathrm{Log}_{10}(Rx)\right)^{2.58} \left(1 + \frac{M_e^2}{5}\right)^{0.467}} = \xi$$

and $$\left(P_L - P_\infty\right) = \psi$$

then the tabulation is as shown in Table III of this Appendix:-

TABLE III

P_L KN/m²	r mm	dx mm	M_e	$\bar{P}$	$\bar{P}r^{\alpha}$	X mm	Rx	ξ N/m	ξdx N	ψ	dA mm²
63.39	57.21	4.57	0.846	0.300	47.23	4.57	6.68×10^4	32.15	0.147	0.30	0
61.02	57.21	9.14	0.882	0.340	53.47	13.18	1.96×10^5	27.07	0.247	-2.07	0
59.60	57.21	9.14	0.904	0.365	57.40	21.40	3.21×10^5	25.25	0.230	-3.49	54.84
58.92	56.90	9.14	0.915	0.377	58.94	30.02	4.53×10^5	23.85	0.218	-4.16	129.36
58.24	56.48	9.14	0.925	0.389	60.32	38.45	5.83×10^5	22.86	0.209	-4.84	204.52
58.31	55.75	9.14	0.924	0.388	59.15	48.40	7.33×10^5	21.65	0.197	-4.77	297.43
59.60	54.78	9.14	0.904	0.365	54.38	61.97	9.28×10^5	20.04	0.183	-3.49	358.08
59.60	53.67	9.14	0.904	0.364	53.00	72.50	1.09×10^6	19.11	0.174	-3.49	437.44
62.64	52.18	9.14	0.857	0.312	43.81	96.80	1.42×10^6	16.91	0.154	-0.44	490.99
63.29	50.67	9.14	0.848	0.301	40.80	113.30	1.65×10^6	15.82	0.145	0.20	499.06
68.13	49.04	8.76	0.774	0.228	29.64	164.60	2.30×10^6	13.16	0.115	5.04	497.44
68.13	47.44	4.95	0.774	0.228	28.44	176.50	2.47×10^6	12.58	0.062	5.04	302.59

$$\int_A \psi \, dA = \int_A \left(P_L - P_\infty\right) dA = -1.98 \text{ N}$$

$$0.6608\pi \int_0^x \xi \, dx = 2\pi \int_0^x r \, \tau \, dx = 4.33 \text{ N}$$

so that $F_c = 6.31$ N

2.2 Calculation of D_c

$$D_c = 2.8\pi \, r_{TE} \, \theta_{TE} \, P_\infty \, M_\infty^2 \left(\frac{M_{TE}}{M_\infty}\right)^{3.2} \left(\frac{1 + \frac{M_\infty^2}{5}}{1 + \frac{M_{TE}^2}{5}}\right)^{4.6} \quad \text{....(35 bis)}$$

and $$\theta_{TE} = 0.036 \left(1 + \frac{M_{TE}^2}{10}\right)^{-0.70} X \, Rx^{-\frac{1}{5}} \quad \text{....(34 bis)}$$

assuming trailing edge conditions are represented by static number 12, we get

$$D_c = 4.98 \text{ N}$$

2.3 Calculation of F_a

Following Section 2.1 of this Appendix we get the tabulation for F_a shown in Table IV.

TABLE IV

P_L KN/m^2	r mm	dx mm	M_e	$\bar{P}$	$\bar{P}r\alpha$	X mm	Rx	ξ N/m	ξdx N	ψ KN/m^2	dA mm^2
95.93	33.70	3.35	0.908	0.368	29.93	3.35	8.04×10^4	31.48	0.105	32.84	53.55
73.75	33.19	6.68	1.131	0.657	52.38	8.59	2.18×10^5	29.40	0.196	10.66	123.87
58.58	32.51	6.68	1.306	0.899	69.82	13.13	3.34×10^5	27.35	0.182	- 4.50	158.07
48.08	31.64	6.68	1.447	1.083	81.27	17.96	4.48×10^5	24.78	0.165	-15.00	183.88
49.00	30.65	6.68	1.434	1.066	76.93	25.65	6.42×10^5	22.59	0.151	-14.08	200.65
53.53	29.56	6.68	1.371	0.986	67.99	35.70	9.02×10^5	20.77	0.138	- 9.54	218.72
70.09	28.29	6.68	1.171	0.713	46.51	58.88	1.50×10^6	18.04	0.120	7.01	236.78
73.07	26.89	6.68	1.138	0.667	40.89	73.66	1.87×10^6	16.38	0.109	9.98	250.33
67.72	25.32	6.68	1.197	0.750	42.58	77.45	1.97×10^6	15.52	0.103	4.64	256.14
54.52	23.67	6.68	1.358	0.969	50.61	71.81	1.82×10^6	14.81	0.099	- 8.56	260.01
69.42	21.81	10.79	1.178	0.723	34.10	117.37	2.99×10^6	12.46	0.134	6.33	405.83

$$\int_A \psi \, dA = \int_A \left(P_L - P_\infty\right) dA = 0.38 \text{ N}$$

$$0.6608 \int_o^x \xi \, dx = 2\pi \int_o^x r \, \tau \, dx = 3.12 \text{ N}$$

so that $F_a = 2.74$ N

In this example, all pressure ratios are supercritical (>1.89) so that

$$D_a = F_a + F_c - D_c$$

$$= 2.74 + 6.31 - 4.98$$

$$= 4.07 \text{ N}$$

and $$\frac{D_a}{F_{ID}} = 0.0064$$

3.0 Example 2 - Intermediate pressure ratio

For the second example, a case where the primary nozzle pressure ratios are on either side of critical has been chosen.

Tunnel	P_T	= 100.80 KN/m^2 abs	Θ_T	=	288 K
Fan stream	P_{Tf}	= 138.68 KN/m^2 abs	Θ_T	=	293 K
Primary stream	P_{Tp}	= 137.63 KN/m^2 abs	Θ_T	=	293 K
Fan nozzle base	P_{bf}	= 65.24 KN/m^2 abs			
Primary nozzle base	P_{bp}	= 75.74 KN/m^2 abs			
Free stream static	P_∞	= 63.02 KN/m^2 abs			

so that

APRF	= 2.126
EPRF	= 2.201
APRP	= 1.817
EPRP	= 2.184
M_∞	= 0.848

Pressure distributions

Fan Cowl		Afterbody	
Static No.	P_L in. KN/m^2 abs	Static No.	P_L in. KN/m^2 abs
1	63.26	1	83.29
2	61.16	2	66.16
3	59.58	3	60.15
4	58.67	4	57.55
5	58.06	5	61.64
6	58.13	6	64.77
7	59.41	7	60.79
8	59.41	8	56.95
9	62.18	9	68.01
10	62.85	10	64.47
11	67.03	11	72.30
12	67.34		

$$\left(Q\sqrt{\Theta_T}\right)_{FAN} = 18.91$$

$$\left(Q\sqrt{\Theta_T}\right)_{PRIM} = 6.015$$

$$F_{ID} = 501.81 \text{ N}$$

Pressure force on fan cowl = - 3.21

Skin friction force on fan cowl = 4.33

$$F_c = 7.54$$

$$D_c = 4.97$$

Pressure force on afterbody = 4.97

Skin friction force on afterbody = 2.69

$$F_a = -2.28$$

Fan stream is supercritical so there is no change of momentum to be taken into account

$$\left(Q\sqrt{\Theta_T}\right)_p \left(18.3 - \left(\frac{V}{\sqrt{\Theta_T}}\right)_{APRP}\right) = 3.23$$

$$P_{Tp}\, A_{ep} \left\{\frac{1}{APRP} - \left(1 - \frac{A_p^*}{A_{ep}}\right)\frac{1}{EPRP} - 0.5283\,\frac{A_p^*}{A_{ep}}\right\} = 3.44$$

whence $D_a = 0.08$

and $\frac{D_a}{F_{ID}} = 0.00016$

4.0 Example 3 - Subcritical pressure ratios

Tunnel	P_T	=	100.78 KN/m^2 abs	Θ_T	=	288 K
Fan stream	P_{Tf}	=	112.68 KN/m^2 abs	Θ_T	=	291 K
Primary stream	P_{Tp}	=	111.92 KN/m^2 abs	Θ_T	=	291 K
Fan nozzle base	P_{bf}	=	65.22 KN/m^2 abs			
Primary nozzle base	P_{bp}	=	75.04 KN/m^2 abs			
Free stream static	P_∞	=	63.10 KN/m^2 abs			

so that

APRF	=	1.727
EPRF	=	1.786
APRP	=	1.553
EPRP	=	1.774
M_∞	=	0.846

Pressure distributions

Fan Cowl		Afterbody	
Static No.	P_L in. KN/m^2 abs	Static No.	P_L in. KN/m^2 abs
1	63.03	1	70.59
2	60.74	2	66.14
3	59.49	3	62.93
4	58.71	4	63.03
5	58.31	5	61.82
6	58.31	6	61.82
7	59.32	7	62.59
8	59.45	8	63.42
9	61.68	9	64.71
10	62.76	10	66.20
11	65.73	11	69.81
12	66.41		

$$\left(Q\sqrt{\Theta_T}\right)_{FAN} = 15.07$$

$$\left(Q\sqrt{\Theta_T}\right)_{PRIM} = 4.66$$

$$F_{ID} = 345.40$$

The integrations give:

Pressure force on fan cowl	=	-4.66
Skin friction force on fan cowl	=	4.35
F_c	=	9.01
D_c	=	4.97
Pressure force on afterbody	=	4.12
Skin friction force on afterbody	=	2.03
F_a	=	-2.10

Now both streams are subcritical, so we compute thrust changes on Jones' basis.

$$\frac{V_{jf}}{\sqrt{\Theta_T}} = 17.53, \qquad \frac{V_{jp}}{\sqrt{\Theta_T}} = 17.432$$

$$\frac{V_{ef}}{\sqrt{\Theta_T}} = 17.054, \qquad \frac{V_{ep}}{\sqrt{\Theta_T}} = 15.418$$

$$\left(Q\sqrt{\Theta_T}\right)_f \left(\frac{V_{jf}}{\sqrt{\Theta_T}} - \frac{V_{ef}}{\sqrt{\Theta_T}}\right) = 7.16$$

$$\left(Q\sqrt{\Theta_T}\right)_p \left(\frac{V_{jp}}{\sqrt{\Theta_T}} - \frac{V_{ep}}{\sqrt{\Theta_T}}\right) = 9.39$$

$$\left(A_{ef}\right)\left(P_{bf} - P_\infty\right) = 7.41$$

$$\left(A_{ep}\right)\left(P_{bp} - P_\infty\right) = 10.13$$

whence $D_a = 0.95$

and $\frac{D_a}{F_{ID}} = 0.003$

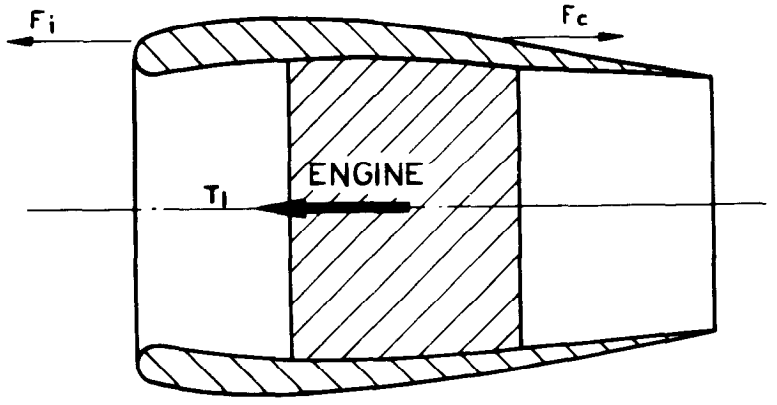

FIG.1a FORCES ON A SINGLE STREAM NACELLE IN ISOLATION

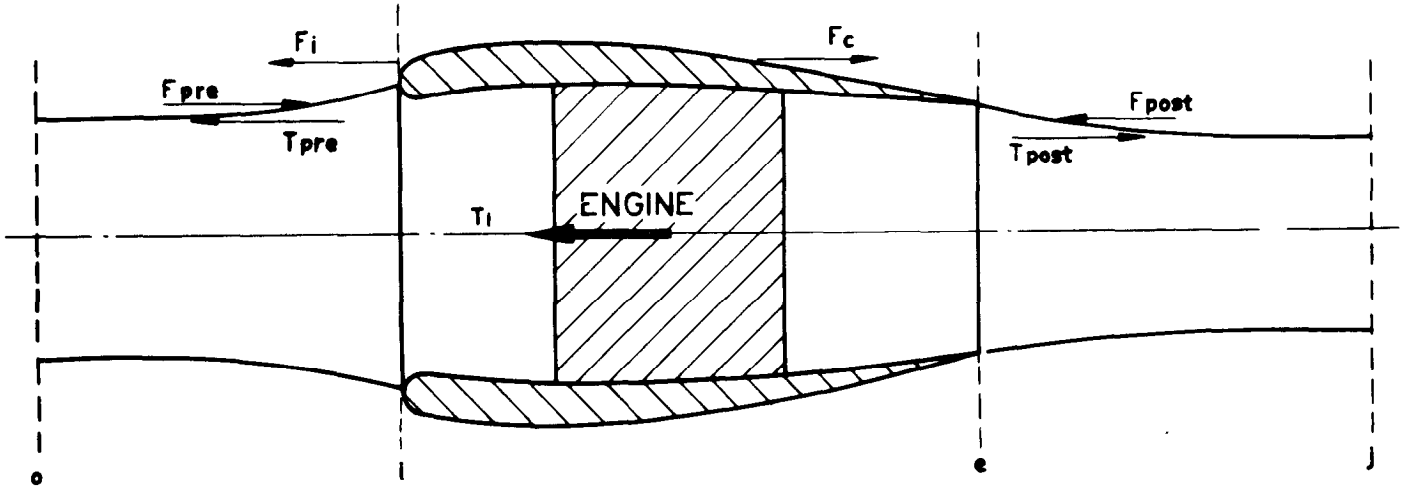

FIG. 1b FORCES USED IN DERIVATION OF THRUST AND DRAG

FIG. 1 THE SINGLE STREAM NACELLE

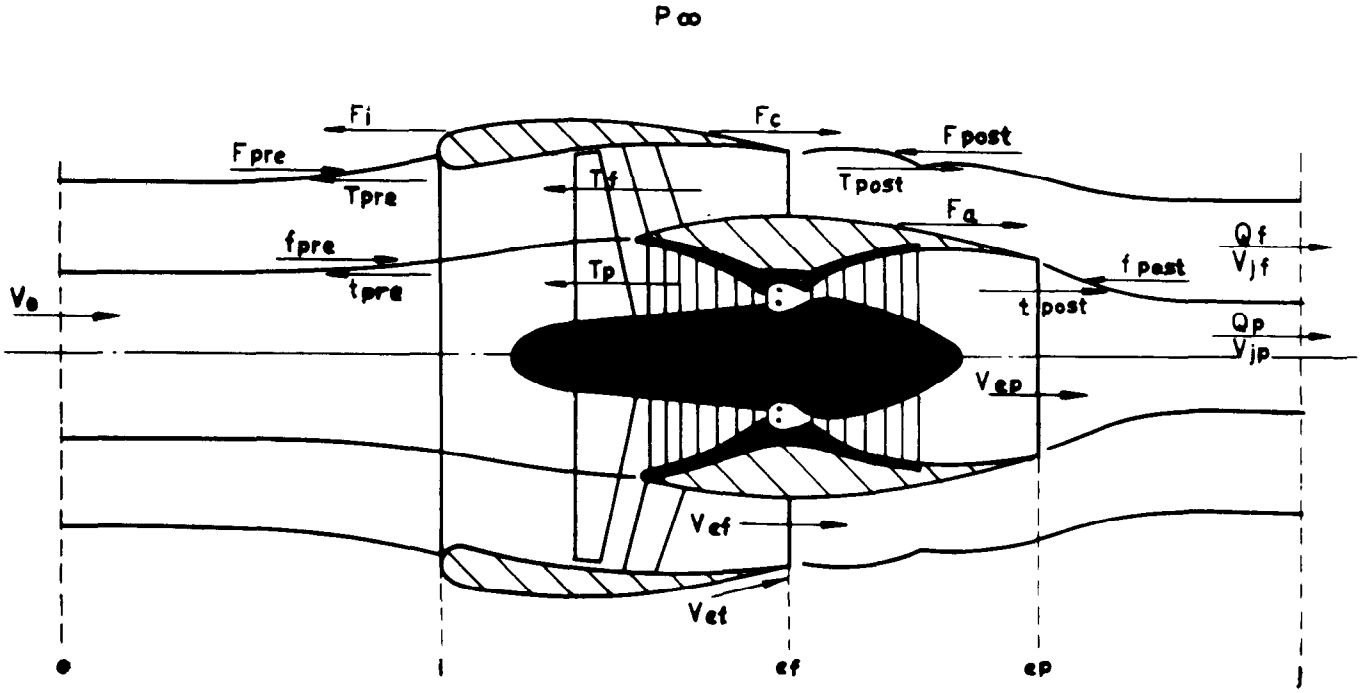

FIG. 2 THE TWO STREAM NACELLE

Produced in England by Her Majesty's Stationery Office, Reprographic Centre, Basildon
R 78852/R54 K4 1/75 P

ARC CP No.1311
February 1973
Street, P.G., NGTE

THRUST/DRAG ANALYSIS FOR A FRONT FAN NACELLE HAVING TWO SEPARATE CO-AXIAL EXHAUST STREAMS

The forces acting on and around a high by-pass ratio front fan nacelle have been considered in the light of the findings of an ARC panel on thrust and drag definitions for jet engines. From these considerations, thrust and drag components which take account of mutual interference have been defined.

A technique for defining an afterbody, or gas generator cowl drag in the presence of external flow is

derived/

ARC CP No.1311
February 1973
Street, P.G., NGTE

THRUST/DRAG ANALYSIS FOR A FRONT FAN NACELLE HAVING TWO SEPARATE CO-AXIAL EXHAUST STREAMS

The forces acting on and around a high by-pass ratio front fan nacelle have been considered in the light of the findings of an ARC panel on thrust and drag definitions for jet engines. From these considerations, thrust and drag components which take account of mutual interference have been defined.

A technique for defining an afterbody, or gas generator cowl drag in the presence of external flow is

derived/

derived and the experimental measurements required are listed. Example calculations using experimental data are used to demonstrate the technique.	derived and the experimental measurements required are listed. Example calculations using experimental data are used to demonstrate the technique.

HER MAJESTY'S STATIONERY OFFICE

Government Bookshops

49 High Holborn, London WC1V 6HB
13a Castle Street, Edinburgh EH2 3AR
41 The Hayes, Cardiff CF1 1JW
Brazennose Street, Manchester M60 8AS
Southey House, Wine Street, Bristol BS1 2BQ
258 Broad Street, Birmingham B1 2HE
80 Chichester Street, Belfast BT1 4JY

Government publications are also available through booksellers

C.P. No. 1311

ISBN 0 11 470895 9